Intelligent Decision Technologies 7 (2013) 3–10
DOI 10.3233/IDT-120147
IOS Press

Brain white matter lesion classification in multiple sclerosis subjects for the prognosis of future disability

Christos P. Loizou[a,*], Efthyvoulos C. Kyriacou[b], Ioannis Seimenis[c,d], Marios Pantziaris[e], Styliani Petroudi[f], Minas Karaolis[f] and Constantinos S. Pattichis[f]
[a]*Department of Computer Science, Intercollege, Limassol, Cyprus*
[b]*Department of Computer Science and Engineering, Frederick University, Limassol, Cyprus*
[c]*Medical Diagnostic Centre "Ayios Therissos", Nicosia, Cyprus*
[d]*Department of Medical Physics, Medical School, Democritus University of Thrace, Alexandroupolis, Greece*
[e]*Cyprus Institute of Neurology and Genetics, Nicosia, Cyprus*
[f]*Department of Computer Science, University of Cyprus, Nicosia, Cyprus*

Abstract. This study investigates the application of classification methods for the prognosis of future disability on MRI-detectable brain white matter lesions in subjects diagnosed with clinical isolated syndrome (CIS) of multiple sclerosis (MS). In order to achieve these we had collected MS lesions from 38 subjects, manually segmented by an experienced MS neurologist, on transverse T2-weighted images obtained from serial brain MR imaging scans. The patients have been divided into two groups, those belonging to patients with EDSS$\leqslant$2 and those belonging to patients with EDSS $>$ 2 (expanded disability status scale (EDSS)) that was measured at 24 months after the onset of the disease). Several image texture analysis features were extracted from the plaques. Using the Mann-Whitey rank sum test at $p < 0.05$ we had identified the features that could give acceptable significant difference. Based on these features three different classification models were investigated for predicting a subject's disability score (two class models, EDSS $\leqslant$ 2 and EDSS $>$ 2). These models were based on the Support Vector Machines (SVM), the Probabilistic Neural Networks (PNN), and the decision trees algorithm (C4.5). The highest percentage of correct classification's score achieved was 69% when using the SVM classifier. The findings of this study provide evidence that texture features of MRI-detectable brain white matter lesions may have an additional potential role in the clinical evaluation of MR images in MS.

Keywords: MRI, multiple sclerosis, texture classification

1. Introduction

Multiple sclerosis (MS) is the most common autoimmune disease of the central nervous system, with complex pathophysiology, including inflammation, demyelination, axonal degeneration, and neuronal loss. Within individuals, the clinical manifestations are unpredictable, particularly with regard to the development of disability [1].

Diagnostic evaluation of MS, performed by a specialized neurologist, is generally based on conventional magnetic resonance imaging (MRI) following the McDonald criteria [2], and on clinical signs and symptoms. The development of modern imaging techniques for the early detection of brain inflammation and the characterization of tissue-specific injury is an important objective in MS research. Recent MRI studies have shown that brain and focal lesion volume measures, magnetization transfer ratio and diffusion weighted imaging-derived parameters can provide new

*Corresponding author: Christos P. Loizou, Department of Computer Science, Intercollege, P. O. Box 51604, CY-3507, Limassol, Cyprus. E-mail: panloicy@logosnet.cy.net.

ISSN 1872-4981/13/$27.50

information in diagnosing MS [3]. Texture features quantify macroscopic lesions and also the microscopic abnormalities that may be undetectable using conventional measures of lesion volume and number [1,4]. Several studies have been published, where it was documented that texture features can be used for the assessment of MS lesions in: (i) differentiating between lesions for normal white matter (NWM), and the so called normal appearing white matter (NAWM) [5–9], and (ii) monitoring the progression of the disease over longitudinal scans [10–14].

Our primary objective in this study is to develop texture classification methods that can be used to predict MS brain lesions that at a later stage are associated with advanced clinical disability and more specifically with the expanded disability status scale (EDSS). Since the use of quantitative MRI analysis as a surrogate measure in clinical trials, we hypothesize that there is a close relationship between the change in the extracted features and the clinical status and the rate of development of disability. We analyzed patient's images acquired at the initial stages of the disease-clinical isolated syndrome (CIS) (0 months) and we correlated texture findings with disability assessment scales. We interrelate therefore the EDSS scores [15] with standard shape and texture features.

The motivation of this study was to investigate the usefulness of classical texture analysis in predicting the progression of the disease as prescribed by the EDSS score. Preliminary findings addressing this problem have also been recently published by our group based on classical texture features [16], as well as multiscale Amplitude Modulation – Frequency Modulation features (AM-FM) [14]. Moreover, the predictive performance of the classical texture features will be contrasted to the AM-FM features.

MRI-based texture analysis was shown to be effective in classifying MS lesions from NWM and the so called, NAWM, with an accuracy of 96%–100% [5]. In [6], the authors showed that texture features can reveal discriminant features for differentiating between normal and abnormal tissue, and for image segmentation. Significant differences in texture between normal and diseased spinal cord in MS subjects were found in [7] as well as a significant correlation between texture features and disability. The median value increase of these texture features suggests that the lesions texture in MS subjects is less homogeneous and more complex than the corresponding healthy tissue (NWM) in healthy subjects [7]. Similar findings were also found in [8,9], where it was shown that median values of lesion texture features such as first and second order texture statistics, standard deviation, median, sum of squares variance, contrast, sum average, sum variance, difference variance, and difference entropy increased significantly with the progression of the MS disease when compared to NWM tissue. Statistical analysis (using the spatial gray level dependence matrices) has shown that there is a significant difference between lesions and NAWM or NWM. These findings may be beneficial in the research of early diagnosis and treatment monitoring in MS.

The differentiation between active and non-active brain lesions in MS subjects from brain MRI was also investigated in [11]. Here, it was shown that active lesions could be identified without frequent gadolinium injections, using run length analysis criteria. In [12] the performance of texture analysis concerning discrimination between MS lesions, NAWM and NWM from healthy controls was investigated by using linear discriminant analysis. The results suggested that texture features can support early diagnosis in MS. When a combined set of texture features was used [12], similar findings were reported.

In [13], a pattern recognition system was developed for the discrimination of MS from cerebral microangiopathy lesions based on computer-assisted texture analysis of MR images. It was shown that, MS regions were darker, of higher contrast, less homogeneous and rougher as compared to cerebral microangiopathy. Finally, in [14], the use of multi-scale AM-FM texture analysis of MS using MR images from brain was introduced. It was shown that the AM-FM features provide complementary information to classical texture analysis features like the gray-scale median, contrast, and coarseness. The findings of this study provide evidence that image texture analysis features may have a potential role as surrogate markers of lesion load in MS.

The paper is organized as follows. Section 2 describes the materials and methods. Section 3 describes the results, and Section 4 presents the discussion.

2. Materials and methods

2.1. Material and MRI acquisition

Thirty eight subjects (17 males, and 21 females), aged 31.4 ± 12.6 (mean age $\pm$ standard deviation) were scanned at 1.5 T within one month following initial clinical evaluation to confirm CIS diagnosis. The transverse MR images used for analysis were obtained us-

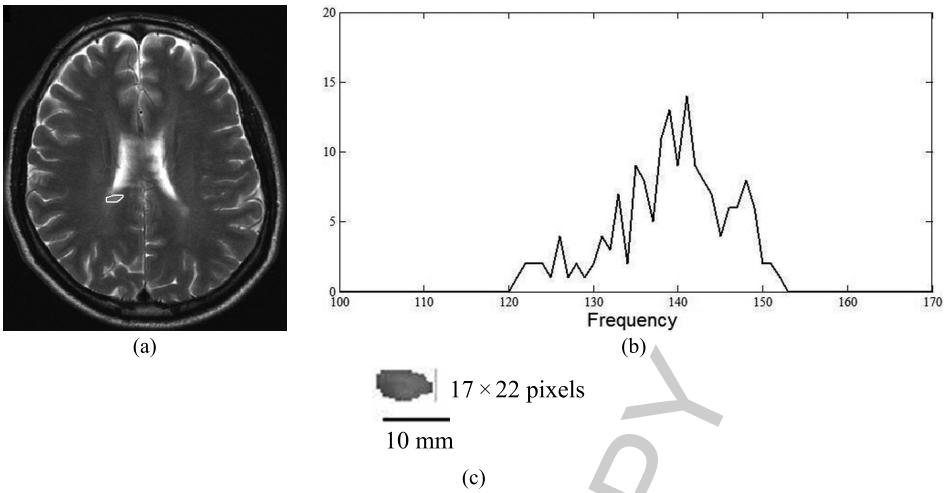

Fig. 1. (a) ROI drawn on MR image of the brain obtained from a 42 year old male MS patient with an EDSS = 3.5 at 0 months, (b) The lesion histogram, and (c) magnified segmented lesion that was acquired at a pixel resolution of 2.226 pixels per mm. The bar below the lesion shows the size of 10 mm. The grey scale median and inter-quartile range (IQR) of the segmented lesion were 139 and 17.2, respectively. The texture feature values as given in Table 1 for this lesion are as follows: mean (138.1), median (139), IDM (0.245), SA (279.56), SRE_03 (0.93), LRE_03 (1.28), SRE_05 (0.48), LRE_05 (4.92), LRE_10 (9.89), GLD_10 (2.96).

ing a T2-weighted turbo spin echo pulse sequence (repetition time = 4408 ms, echo time = 100 ms, echo spacing = 10.8 ms). The reconstructed image had a slice thickness of 5 mm and a field of view of 230 mm with a pixel resolution of 2.226 pixels per mm. Standardized planning procedures were followed during each MRI examination. The MRI protocol and the acquisition parameters were given in detail in [8,9].

Initial clinical evaluation was made by an experienced MS neurologist (co author M.P.) who referred subjects for a baseline MRI upon diagnosis and clinically followed all subjects for over two years. All subjects were subjected to an EDSS test two years after initial diagnosis to quantify disability [15]. They were clinically followed and examined by an MS neurologist (co-author M.P.) following the initial MRI and also at two years later. At the initial scan, the stage of the disease was evaluated using the EDSS score [15]. The subjects were referred for the MRI scans to Ayios Therissos Medical Diagnostic Centre (co-author, I.S.).

A normalization algorithm was used to match the image brightness between the first (baseline) and the follow-up images (see [16] for details). For this purpose, the neurologist manually segmented cerebrovascular fluid (CSF) areas as well as areas with air (sinuses) from all MS brain scans. Similarly, regions of interest (ROIs) representing NWM, CSF and air from the sinuses were arbitrarily segmented from the brain scans of 20 healthy subjects. The original image histogram was stretched, and shifted in order to cover all the gray scale levels in the image.

To introduce the objective of our study, an example in Fig. 1(a) is presented. Here, we show a transaxial T2-weighted MR image of a male patient at the age of 42, with an EDSS [15] equal to 3.5. The image in Fig. 1 corresponds to the initial diagnosis of a CIS of MS and the delineated lesion corresponding to the MS plaque is also depicted. Figure 1(b) presents the lesions histogram, whereas Fig. 1(c) shows the magnified segmented lesion from Fig. 1(a) (original images were acquired at a sampling rate of 2.226 pixels per mm). In what follows, texture analysis refers to the image processing of the extracted ROIs.

2.2. Manual delineations and visual perception

All MRI-detectable brain lesions were identified and segmented by an experienced MS neurologist and confirmed by a radiologist. Only well-defined areas of hyperintensity on T2-weighted MR images were considered as MS lesions. The neurologist manually delineated (using the mouse) the brain lesions by selecting consecutive points at the visually defined borders between the lesions and the adjacent NAWM on the acquired transverse T2-weigted sections. Similar regions corresponding to NAWM were delineated contra laterally to the detected MS lesions. The manual delineations were performed using a tool developed by our group using MATLAB® software. Manual segmentation by the MS expert was performed in a blinded manner, without the possibility of identifying the subject

or the clinical findings. The selected points and delineations were saved to be used for texture analysis.

2.3. Texture analysis

In this study texture features and shape parameters were extracted from all MS lesions detected and segmented [8,9]. The overall texture and shape features for each subject were then estimated by averaging the corresponding values for all lesions for each subject. The following texture features were extracted: (i) Statistical Features (SF): a) mean, b) variance, c) median value, d) skewness, e) kurtosis, f) energy and g) entropy. (ii) Spatial Gray Level Dependence Matrices (SGLDM) as proposed by Haralick et al. [17]: a) angular second moment (ASM), b) contrast, c) correlation, d) sum of squares variance (SOSV), e) inverse difference moment (IDM), f) sum average (SAV), g) sum variance (SV), h) sum entropy (SENT), i) entropy (ENT), j) difference variance (DVAR), k) difference entropy (DENT), and l) information measures of correlation (IMC). For a chosen distance d (in this work d $= 1$ was used) and for angles $\theta = 0°$, 45°, 90°, and 135°, we computed four values for each of the above texture measures. Each feature was computed using a distance of one pixel. Then for each feature the mean values and the range of values were computed, and were used as two different features sets. (iii) Gray Level Difference Statistics (GLDS) [18]: a) homogeneity, b) contrast, c) energy, d) entropy, and e) mean. The above features were calculated for displacements $\delta = (0, 1)$, (1, 1), (1, 0), (1, -1), where $\delta \equiv (\Delta x, \Delta y)$, and their mean values were taken. (iv) Neighborhood Gray Tone Difference Matrix (NGTDM) [19]: a) coarseness, b) contrast, c) busyness, d) complexity, and e) strength. (v) Fractal Dimension Texture Analysis (FDTA) [21]: The Hurst coefficients for dimensions 4, 3 and 2 were computed. (vi) Fourier Power Spectrum (FPS) [1,18]: a) radial sum, and b) angular sum. (vii) Gray Level Run Length Statistics (RUNL) [20]: a) Short Run Emphasis (SRE), b) Gray Level Distribution (GLD), Run Length Distribution (RLD), Long Run Emphasis (LRE), Run Percentage (RP). These features were calculated using a modification on the algorithm, were the differences of the gray levels were not just tested for 0 but also for a difference of 3, 5, 10, 15 and 20. (viii) Shape Parameters: a) X–coordinate maximum length, b) Y–coordinate maximum length, c) area, d) perimeter, e) perimeter2/area, f) eccentricity, g) equivalence diameter, h) major axis length, i) minor axis length, j) centroid, k) convex area, and l) orientation.

2.4. Classification models

Classification analysis was carried out to classify brain MS lesions delineated on the baseline MRI scans into two classes according to the EDSS score that each patient was allocated two years following initial diagnosis: (i) MS subjects with EDSS $\leqslant 2$, and (ii) MS subjects with an EDSS > 2. Thus, the classification goal was to differentiate between lesions that were subsequently associated with mild (EDSS $\leqslant 2$) or advanced disability (EDSS > 2). The classification was applied on 38 subjects (17 males and 21 females).

Modeling was carried out using three different classifiers: the Support Vector Machine (SVM), the Probabilistic Neural Network (PNN), and the decision trees classification based on the C4.5 algorithm.

2.4.1. The support vector machines classifier

The Support Vector Machines (SVM) method is initially based on a nonlinear mapping of the initial data set using a function $\varphi(.)$ and then the identification of a hyperplane which is able to achieve the separation of two categories of data. The vectors defining the hyperplanes can be chosen to be linear combinations with parameters α_i of images of feature vectors that occur in the data base. With this choice of a hyperplane, the points x in the feature space that are mapped into the hyperplane are defined by the relation:

$$\sum \alpha_i K(x_i, x) = \textit{constant} \quad (1)$$

If $K(x, y)$ becomes small as y grows further from x, each element in the sum measures the degree of closeness of the test point x to the corresponding data base point x_i. In this way, the sum of kernels above can be used to measure the relative nearness of each test point to the data points originating in one or the other of the sets to be discriminated.Details about the implementation of the SVM algorithm used can be found in [23–25]. The files used are the Matlab® interface to SVMlight [23] written by Anton Schwaighofer. The SVM network was investigated using Gaussian Radial Basis Function (RBF) kernels and a C parameter of 1; this was decided as the rest of the kernel functions could not achieve satisfactory results. The data set was divided into 10 bootstrap sets of 30 cases each (15 cases from each class) selected at random. On each one of these sets the SVM with the RBF kernel was investigated in order to identify the best parameter settings such as the spread of the RBF. The validation was performed also on each of the 10 bootstrap sets in order to validate the classification success rate. This was done using the leave-one-out estimate. The mean value of the 10 runs was computed.

2.4.2. The probabilistic neural network classifier

The Probabilistic Neural Network (PNN) [25] classifier was used for developing classification models for the problem under study. The PNN falls within the category of nearest-neighbor classifiers. For a given vector $\mathbf{w}$ to be classified, an activation a_i is computed for each of the two classes of plaques ($i = 1, 2$). The activation a_i is defined to be the total distance of $\mathbf{w}$ from each of the M_i prototype feature vectors $\mathbf{x}_j^{(i)}$ that belong to the i-th class:

$$a_i = \sum_{j=1}^{M_i} \exp\left[-\beta \left(\mathbf{w}-\mathbf{x}_j^{(i)}\right)^T \left(\mathbf{w}-\mathbf{x}_j^{(i)}\right)\right], \qquad (2)$$

where β is a smoothing factor. This classifier was investigated using the corresponding Matlab® function with the default spread radii equal to 0.1 [26]. The networks investigated were two layer. The first layer had radial basis function neurons, computed similar to the SVM neurons described in Section 2.4.1. The second layer had competitive transfer function neurons [26]. The PNN classifier models were trained and evaluated similar to the SVM models described in Section 2.4.1 above.

2.4.3. The C4.5 algorithm

The C4.5 algorithm, which uses the divide-and-conquer approach to decision tree induction was employed [27]. The algorithm uses a selected criterion to build the tree. In this study, the information gain splitting criterion was investigated. It works top-down, seeking at each stage an attribute to split on that which best separates the classes, and then recursively processing the sub problems that result from the split. The algorithm uses heuristics for pruning, derived based on the statistical significance of splits. The WEKA implementation of the C4.5 algorithm was used [28].

In WEKA tool [29] the C4.5 algorithm is defined as J48. We changed the parameter *confidenceFactor* to 0.25 and *minMumObj* to 2. The values of the other parameters were the default WEKA values. The classifier was run using the attribute *Class*, which has two values: the value L for the patients with EDSS $\leqslant 2$ and the value H for the patients with EDSS > 2. The testing option was 10-fold cross validation.

2.5. Classification models performance evaluation

The performance of the prediction models was measured using the receiver operating characteristics (ROC) curve parameters [30]. The parameters calculated were the following: (i) true positives (TP) when the model correctly classifies subjects as EDSS $\leqslant 2$, or EDSS > 2, (ii) false positives (FP) when the model wrongly classifies subjects as EDSS > 2 while they belong in the group of EDSS $\leqslant 2$, (iii) true negatives (TN) when the model correctly classifies subjects as EDSS $\leqslant 2$. We also computed the Sensitivity (SE) which is the likelihood that a subject with EDSS > 2 will be detected given that it is EDSS > 2 and Specificity (SP) which is the likelihood that a subject will be classified as EDSS $\leqslant 2$ given that he/she is EDSS $\leqslant 2$. For the overall performance, we provide the correct classifications (CC) score which gives the percentage of correctly classified subjects.

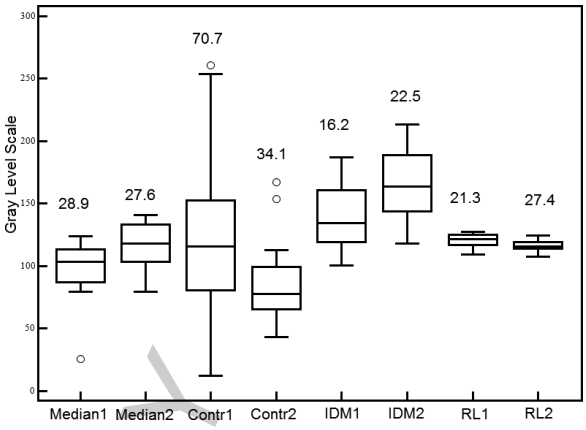

Fig. 2. Box plots for the median ± inter-quartile range (IQR) values for texture features median, contrast, IDM (×500), and RUNL_05_LRE (RL) (×150), from MS lesions at 0 months for EDSS $\leqslant 2$ (N = 23) and EDSS > 2 (N = 15) corresponding to feature notation 1, and 2 respectively (see also Table 1). IQR values are shown above the box plots. In each plot we display the median, lower, and upper quartiles and confidence interval around the median. Straight lines connect the nearest observations within 1.5 of the IQR of the lower and upper quartiles.

3. Results

Figure 2 presents the box plots of the lesion texture features median, contrast, IDM (×500), and RUNL_05_LRE (RL) (×150), for the MRI lesions with EDSS $\leqslant 2$ (1) (N = 23) and EDSS > 2 (2) (N = 15). Table 1 tabulates the median and Inter Quartile Range (IQR) for the statistically significant features only based on the Mann-Whitney rank sum test at $p < 0.05$. The features tabulated are the Statistical Features: mean and median, the Spatial Gray Level Dependence Matrices: IDM, and SA, and the Gray Level Run Length Statistics: short run emphasis with 3 and 5 grey level differ-

Table 1
Statistical analysis of the texture features for lesions with EDSS $\leqslant 2$ (N = 23) and EDSS > 2 (N = 15). The median and Inter Quartile Range (IQR) are given only for the statistically significant features based on the Mann-Whitney rank sum test at $p < 0.05$. Significant difference is depicted with S and non significant difference is depicted with NS

Feature	Lesions with EDSS $\leqslant 2$ median (IQR)	Lesions with EDSS > 2 median (IQR)	Mann-Whitney rank sum test
Statistical Features (SF)			
Mean	104 (26)	121 (28.5)	S (0.03)
Median	103 (25)	118 (30)	S (0.03)
Spatial Gray Level Dependence Matrices (SGLDM)			
IDM	0.14 (0.03)	0.16 (0.05)	S (0.01)
Sum average (SA)	213 (54)	246 (57)	S (0.04)
Gray Level Run Length Statistics (RUNL)			
SRE_03	0.8 (0.05)	0.77 (0.038)	S (0.019)
LRE_03	2.4 (0.78)	2.83 (1.03)	S (0.019)
SRE_05	0.71 (0.06)	0.66 (0.05)	S (0.024)
LRE_05	3.83 (1.68)	4.77 (2.04)	S (0.013)
LRE_10	8.79 (5.2)	12.66 (6.52)	S (0.018)
GLD_10	1.77 (0.46)	1.91 (0.46)	S (0.030)

IDM: Inverse difference moment, RUNL: Run length for 3, 5,10,15,20 differences, SRE: Short Run Emphasis with 3 and 5 grey level difference,LRE: Long Run Emphasis with 3, 5, and 10 grey level difference, GLD: Gray Level Distribution with 10 grey level difference.

Table 2
Prediction model results for two classes: EDSS $\leqslant 2$ and EDSS > 2 based on the features tabulated in Table 1. Performance measures (mean $\pm$ standard deviation) are given for 10 bootstrapping sets (with the leave-one out method used for evaluation) of 15 cases with EDSS $\leqslant 2$ and 15 cases with EDSS > 2 for the Support Vector Machines (SVM) and the Probabilistic Neural Networks (PNN) classifiers. For the C4.5 classifier, 10 fold cross validation was used with five cases with EDSS $\leqslant 2$ and five cases with EDSS > 2 drawn at random from the corresponding 15 cases for each class for each set

Prediction model	%Correct classifications	%Sensitivity	%Specificity	%False negatives	%False positives
SVM	69±3.1	74±7.3	65±10	26±7.3	35±10
PNN	63±4.6	60±4.4	66±6.6	40±4.4	34±6.6
C4.5	61±9.9	64±6	59±4	50±22	28±14

ence, long run emphasis with 3, 5, and 10 grey level difference, and gray level distribution with 10 grey level difference. As demonstrated in Fig. 2, and Table 2, both the median and IDM increase with the disability score, whereas the reverse is true for contrast and long run emphasis with 5 grey level difference.

Table 2 tabulates the prediction model results for two classes: EDSS $\leqslant 2$ and EDSS > 2 based on the statistically significant features given in Table 1. Performance measures (mean $\pm$ standard deviation) are given for 10 bootstrapping sets of 15 cases with EDSS $\leqslant 2$ and 15 cases with EDSS > 2 drawn at random from the corresponding 23 cases with EDSS $\leqslant 2$, and 15 cases with EDSS > 2. For the Support Vector Machines (SVM) and the Probabilistic Neural Networks (PNN) models the leave one out method was used for evaluation (i.e. a total of 300 runs were carried out for each prediction model). For the C4.5 five cases with EDSS $\leqslant 2$ and five cases with EDSS > 2 were drawn at random from the corresponding 15 cases for each class (i.e. a total of 10 runs were carried out). The best percentage of correct classifications score was 69±3.1%, and was obtained using the SVM model. The PNN and C4.5 models gave lower percentage of correct classifications score, 63±4.6%, and 61±9.9%, respectively.

4. Discussion

The objective of our study was to investigate texture classification analysis in an effort to differentiate between MS brain lesions that, in a subsequent stage, will be associated with advanced diseased disability from those lesions that will be related to a mild disability score.

Table 1 showed that there are some texture features that can be possibly used to differentiate between subjects with mild (EDSS $\leqslant 2$) and advanced (EDSS > 2) MS disease states. These features are mean, median, IDM, SA, short run emphasis with 3 and 5 grey level difference, long run emphasis with 3, 5, and 10 grey level difference, and gray level distribution with 10 grey level difference. Table 2 showed that these texture features gave a percentage of correct classifications score of 69±3.1%, when classifying subjects according to their long-term disability status.

These results can be compared with another study carried out by our group [14], where amplitude modulation-frequency modulation (AM-FM) feature analysis was used. The objective of the study in [14], was to investigate whether changes in AM-FM characteristics can be associated with MS disease progression. AM-FM features were extracted and investigated based on statistical measures, univariate statistical analysis and SVM based classification analysis. Image analysis was based on the manually segmented MS lesions from the MRI scans of the brain of 38 subjects with CIS, and the NAWM areas from the same MRI scans of the brain of the same patients were used in an attempt to quantify pathological changes that occur in MS. The population sample used in our study represents more than 50% of CIS cases diagnosed in the Cypriot population within the time span of two years. All subjects were scanned twice with an interval of 6–12 months. The findings of our study in [14], suggested that AM-FM characteristics succeeded in differentiating (i) between NWM and lesions, (ii) between NAWM and lesions, and (iii) between NWM and NAWM. The SVM classifier succeeded in differentiating between patients that, two years after the initial MRI scan, acquired an EDSS $\leqslant 2$ from those with EDSS > 2 (correct classification rate $= 86\%$). The best classification results were obtained from including the combination of the low-scale instantaneous amplitude (IA) and instantaneous frequency (IF) magnitude with the medium-scale IA. Among all AM-FM features, the medium frequency IA histogram alone gave the best AUC results (AUC $= 0.76$). Also the best % of correct classifications rate achieved in [14], using the IA histograms from all frequency scales of the AM-FM features, was 86%. The best classifier results also used the IF magnitude from both the low and the high frequency scales.

To the best of our knowledge, no other studies were carried out for differentiating between the aforementioned two disability scores. Several studies were carried out for differentiating and classifying NWM, and or NAWM, from lesions, as these are outlined in the introduction section.

Concluding, the findings of this study provide evidence that texture features of MRI-detectable brain white matter lesions may have an additional potential role in the evaluation of MRI images in MS and the prediction of disability. However these findings have to be evaluated in more subjects and in more MS clinics.

Acknowledgments

This work was partially funded through the project "Quantitative and Qualitative Analysis of MRI Brain Images" $\mathrm{TIIE/OPIZO/0308(BIE)/15}$, 12/2008–12/2010, of the Program for Research and Technological Development 2007–2013, co funded by the Research Promotion Foundation of Cyprus and the "European Regional Development Fund".

References

[1] F. Fazekas, F. Barkof, M. Filippi, R.I. Grossman, D.K.B. Li, W.I. McDonald, H.F. McFarland, D.W. Patty, J.H. Simon, J.S. Wolinsky and D.H. Miller, The contribution of magnetic resonance imaging to the diagnosis of multiple sclerosis, *Neur* **53** (1999), 448–456.

[2] W.I. McDonald, A. Compston, G. Edan et al., Recommended diagnostic criteria for multiple sclerosis: Guidelines from the international panel on the diagnosis of multiple sclerosis, *Ann Neurol* **50** (2001), 121–127.

[3] R. Bakshi, A.J. Thompson, M.A. Rocca et al., MRI in multiple sclerosis: Current status and future prospects, *Lancet Neurol* **7** (2008), 615–625.

[4] A. Kassner and R.E. Thornhill, Texture analysis: A review of neurologic MR imaging applications, *Am J Neuroradiol* **31** (2010), 809–816.

[5] L.C.V. Harrison, M. Raunio, K.K. Holli, T. Luukkaala, S. Savio et al., MRI Texture analysis in multiple sclerosis: Toward a clinical analysis protocol, *Acad Radiol* **17** (2010), 696–707.

[6] S. Herlidou-Meme, J.M. Constans, B. Carsin, D. Olivie, P.A. Eliat et al., MRI texture analysis on texture test objects, normal brain and intracranial tumors, *Mag Res Imag* **21** (2003), 989–993.

[7] J.M. Mathias, P.S. Tofts and N.A. Losseff, Texture analysis of spinal cord pathology in multiple sclerosis, *Magn, Reson Med* **42** (1999), 929–935.

[8] C.P. Loizou, C.S. Pattichis, I. Seimenis, E. Eracleous, C.N. Schizas and M. Pantziaris, Quantitative analysis of brain white matter lesions in multiple sclerosis subjects: Preliminary findings, *IEEE Proc,* 5^{th} *Int Conf Inf Techn Appl Biomed, ITAB*, Shenzhen, China, (30–31 May 2008), 58–61.

[9] C.P. Loizou, C.S. Pattichis, I. Seimenis and M. Pantziaris, Quantitative analysis of brain white matter lesions in multiple sclerosis subjects, 9^{th} *Int Conf Inform Techn Applic Biomed, ITAB*, Larnaca, Cyprus (5–7 Nov 2009), 1–4.

[10] G. Collewet, M. Strzelecki and F. Marriette, Influence of MRI acquisition protocols and image intensity normalization methods on texture classification, *Magn Reson Imag* **22** (2004), 81–91.

[11] O. Yu, Y. Mauss, G. Zollner, I.J. Namer and J. Chambron, Distinct patterns of active and non-active plaques using texture analysis of brain NMR images in multiple sclerosis patients: Preliminary results, *Magn Reson Imag* **17**(9) (1999), 1261–1267.

[12] J. Zhang, L. Wang and L. Tong, Feature reduction and texture classification in MRI-Texture analysis of multiple sclerosis, *IEEE/ICME Conf Complex Med Eng* (2007), 752–757.

[13] D.S. Meier and C.R.G. Guttman, Time-series analysis of MRI intensity patterns in multiple sclerosis, *NeuroImage* **20** (2003), 1193–1209.
[14] C.P. Loizou, V. Murray, M.S. Pattichis, I. Seimenis, M. Pantziaris and C.S. Pattichis, Multi-scale Amplitude Modulation-Frequency Modulation (AM-FM) texture analysis of multiple sclerosis in brain MRI images, *IEEE Trans Inform Tech Biomed* **15**(1) (2011), 119–129.
[15] A.J. Thompson and J.C. Hobart, Multiple sclerosis: Assessment of disability and disability scales, *J Neur* **254**(4) (1998), 189–196.
[16] C.P. Loizou, E.C. Kyriacou, I. Seimenis, M. Pantziaris, C. Christodoulou and C.S. Pattichis, Brain white matter lesions classification in multiple sclerosis subjects for the prognosis of future disability, *Artificial Intelligence Applications and Innovations, 12th INNS EANN-SIG International Conference, EANN 2011 and 7th IFIP WG 12.5 International Conference, AIAI 2011, (IFIP Advances in Information and Communication Technology)*, Corfu, Greece **364** (15–18 September 2011), 400–409.
[17] R.M. Haralick, K. Shanmugam and I. Dinstein, Texture features for image classification, *IEEE Trans Syst, Man, and Cybernetics* **SMC-3** (1973), 610–621.
[18] J.S. Weszka, C.R. Dyer and A. Rosenfield, A comparative study of texture measures for terrain classification, *IEEE Trans Syst, Man Cybern* **SMC-6** (1976), 269–285.
[19] M. Amadasun and R. King, Textural features corresponding to textural properties, *IEEE Trans Syst, Man Cybern* **19**(5) (1989), 1264–1274.
[20] M.M. Galloway, Texture classification using gray level run lengths, *Comp Graph and Imag Proc* **4** (1975), 172–179.
[21] B.B. Mandelbrot, The Fractal Geometry of Nature, San Francisco, CA: Freeman, 1982.
[22] W.H. Press, S.A. Teukolsky, W.T. Vetterling and B.P. Flannery, Section 16.5. Support Vector Machines, *Numerical Recipes: The Art of Scientific Computing* (3rd ed.), New York: Cambridge University Press, ISBN 978-0-521-88068-8, 2007.
[23] http://svmlight.joachims.org/old/svm_light_v4.00.html.
[24] T. Joachims, in: *Making large-Scale SVM Learning Practical*, Chapter 11, Advances in Kernel Methods – Support Vector Learning, B. Schölkopf and C. Burges and A. Smola, eds, MIT Press, 1999.
[25] D.F. Specht, Probabilistic neural networks, *INNS Neural Networks* **3**(1) (1990), 109–118.
[26] P.D. Wasserman, Advanced Methods in Neural Computing, New York: Van Nostrand Reinhold, (1993), 35–55.
[27] J.R. Quinlan, C4.5: Programs for Machine Learning, Morgan Kaufmann Publishers, 1993.
[28] I. H. Witten, E. Frank and M. A. Hall, Data mining: Practical machine learning tools and techniques (third edition), Morgan Kaufmann (2011).
[29] http://weka.wikispaces.com/.
[30] R.C. Ebrchart and R.W. Dobbins, Neural Networks PC Tools, A Practical Guide, Academic Pr. (1990).